

# DYNAMIC STABILITY ANALYSIS OF A HYDROFOILING SAILING BOAT USING CFD

A. Bagué, Ghent University, Belgium, alec.bague@ugent.be.

E. Lataire, Ghent University, Belgium, evert.lataire@ugent.be.

T. Demeester, Ghent University, Belgium, toon.demeester@ugent.be.

J. Degroote, Ghent University, Belgium, joris.degroote@ugent.be.

This paper describes the study of the dynamic stability of a hydrofoiling sailing boat called the “*Goodall Design Foiling Viper*”. The goal of *Goodall Design* is to make hydrofoiling accessible to a wider public, whereas it was previously reserved for professional sailors at the highest level of the sport. To allow for safe operation, stability is an essential characteristic of the boat. The aim of this work is to find a strategy to perform a dynamic stability analysis using computational fluid dynamics (CFD), which can be used in a preliminary design stage. This paper starts by establishing a theoretical framework to perform the dynamic stability analysis. A stability analysis has to be performed around an equilibrium state which depends on operating parameters such as speed, centre of gravity, etc. . A fluid-structure interaction strategy is applied to determine these equilibrium states. The last part discusses the stability characteristics of the Viper. The framework managed to asses the dynamic stability of the Viper and found 5 longitudinal eigenmodes: two complex conjugated pairs of eigenvalues and one real eigenvalue. It can be concluded that the boat was both statically and dynamically stable.

## NOMENCLATURE

Symbol	Definition	(unit)
$x, y, z$	position variables	(m)
$\phi, \theta, \psi$	Euler angles	(rad)
$u, v, w$	velocity	( $m.s^{-1}$ )
$p, q, r$	angular velocity	( $rad.s^{-1}$ )
$F_x$	Force in the x-direction	(N)
$S(t)$	time-dependent state-vector	(-)
$A$	stability matrix	(-)
$m$	mass	(kg)
$I_{yy}$	mass moment of inertia	( $kg.m^2$ )
$\alpha$	angle of attack	(rad.)
$u_0$	equilibrium state forward velocity	( $m.s^{-1}$ )

## 1 INTRODUCTION

In this paper the development of a framework for performing a dynamic stability analysis for a hydrofoiling (sailing) boat will be discussed. This framework will then be applied to the “*Goodall Design Foiling Viper*”[1] (hereafter called Viper). Hydrofoiling is the practice where a normally buoyant vessel is fitted with lifting

surfaces below the water surface which generate an upwards force. This lift will then partly or completely replace the buoyant force of the hull. If this force becomes sufficiently large, it will lift the hull out of the water as if the boat were flying. As the hull is lifted from the water, there is an ensuing reduction of the drag as now only the hull’s appendages are (partly) submerged. This is a clear advantage as it allows for greater speeds for the same propulsive power.

Although being around for a long time, hydrofoils have experienced a recent renaissance in terms of interest and development. They were initially introduced at the highest level of the sailing sport, but today there is an urge to make this development accessible to a wider public. Multiple production classes are already fitted with hydrofoils. The increase in speed and the different way of sailing has however led to new and greater risks: various accidents have already occurred [2]. In the pursuit of making foiling more widely available, safety is one of the primary concerns.

One way of providing sufficient safety is to examine and improve the stability of hydrofoil boats as this will lead to more predictable behaviour and easier handling. The

aim of this work is thus to develop a framework for assessing the dynamic stability of a hydrofoil craft which will allow to compare different designs under various conditions. This framework is aimed to be a useful tool for the preliminary design stage of hydrofoil boats and consequently it should be a tool which is straightforward and fast to use.

The Viper is a 16 feet (5 meter) long multihull, origi-



Figure 1: The Goodall Design Foiling Viper hovering above the water.

nally designed by Greg Goodall in 2007 as a non-foiling high-performance multihull [1]. Because of its light and versatile design it was perfectly suited to be converted to a foiling boat. A picture of the Viper while foiling can be found in Fig. 1. The original, non-foiling Viper has -just like regular multihulls- two straight rudders for steering situated at the back of the boat and two straight daggerboards to limit the drift towards the middle of the boat. To enable foiling, a smaller, horizontal symmetric foil is added to the bottom of both rudders to form a T-shaped rudder. Additionally the straight daggerboards are replaced by a Z-shaped daggerboard. A picture of this setup can be found in Fig. 2. The vertical *stem* of the rudder will from here on be called the *rudder*, the horizontal symmetric foil at its bottom the *elevator* and the daggerboard the *Z-board*. The principle of the setup of the Viper (and other foilers) is very similar to that of a regular aeroplane. The two Z-boards provide the necessary lift near the centre of gravity, the two elevators are placed further downstream to enable stable flight, and the two rudders are there both for active steering and directional stability.

## 2 STABILITY DYNAMICS

The dynamic stability analysis gives quantitative results about the expected stability behaviour of a design in specific conditions or for a range of conditions. These re-

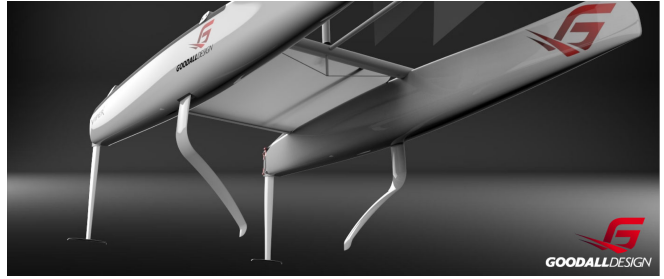


Figure 2: Details of the Viper's foils.

sults can then be used to compare different designs and help make design choices. This analysis also allows to predict the dominant motions the boat will experience. As the literature on dynamic stability of hydrofoil boats is rather limited and the core principles of a hydrofoil boat are very similar to those of an aeroplane, the development of the framework can be based on the theory developed for aeroplanes. This theory is described in many works, such as Drela's work on "Flight Vehicle Aerodynamics" [3]. One of the only sources on dynamic stability analysis specifically for hydrofoil boats is the work by Masuyama [4]. In Sec. 2.1 a general overview will be given, Sec. 2.2 will get into more detail on the used simplifications and the specific framework will be laid out in Sec. 2.3.

### 2.1 GENERAL APPROACH

There are 12 equations governing the motion of the boat: 6 kinematic equations and 6 dynamic equations. More background on how to derive these equations can be found in Drela or Caughey ([3], [5]). Kinematic relations describe the movements of the boat without considering the forces where dynamic relations do consider these. These 12 equations are used to determine 12 *motion variables*. The *state-vector*  $S(t)$  is a combination of these 12 motion variables and contains the position, rotation, velocity and angular velocity of the boat. These variables are then grouped to form a longitudinal ( $u, w, q, \theta$ ), lateral ( $v, p, r, \phi$ ) and navigational ( $x, y, z, \psi$ ) set as can be seen below.

$$S(t) = \{u \ w \ q \ \theta \ v \ p \ r \ \phi \ x \ y \ z \ \psi\}^T$$

The boat is assumed to experience a small disturbance from an original equilibrium state. This equilibrium state is state where the boat is statically stable. Due to this disturbance every term gets perturbed. This gets expressed by substituting every term in the 12 equations by its equilibrium value (denoted with subscript 0) plus

a deviation from this equilibrium value (denoted as a  $\Delta$  term). This is demonstrated in Eq. 1 for the vertical position  $z$ .

$$z(t) = z_0 + \Delta z(t) \quad (1)$$

Forces and moments are functions of the flow-field around the boat. In order to make the equations of motion solvable, the forces and moments have to be expressed as a function of the 12 motion variables. The forces and moments are approximated using a first-order Taylor expansion. This is demonstrated in Eq. 2 for the longitudinal horizontal force  $\Delta F_X$ :

$$\Delta F_X = \sum_i \frac{\partial F_X}{\partial a_i} \Delta a_i \quad (2)$$

with  $a = u, w, q, \theta, v, p, r, \phi, x, y, z, \psi$

The individual derivatives in this expression are called the *force derivatives*, where some can be omitted depending on the situation. Using the state-vector  $S(t)$ , a matrix notation for the equations of motion can be found. This notation is shown in Eq. 3 where  $A$  is the so-called stability matrix which contains the *stability derivatives*. These stability matrix are based on the force derivatives mentioned above.

$$\frac{d}{dt} S(t) = A \cdot S(t), \quad A \in \mathbb{R}^{12 \times 12} \quad (3)$$

When using the grouped state-vector as explained above, where longitudinal, lateral and navigational variables are grouped, the stability matrix gets a structure as laid out in Eq. 4. This matrix can be understood as follows: a row represents a certain element from the time derivative of the state-vector and the columns represent the influencing variables. In the classical theory used for aeroplanes all the terms denoted with a dot ( $\cdot$ ) are the non-zero terms. It can be seen how in that case the longitudinal and lateral subset are decoupled from one-another [3]. The navigational subset (last four rows) does get influenced by the other two subsets. This matrix is singular but we only investigate the non-singular subset. On the other hand we have the terms denoted with a star (\*), which are the additional terms which are non-zero in the general case of a hydrofoil sailing boat. This can be accounted to a variety of reasons, one being the presence of the free-water surface and the ensuing dependency on the draft/elevation  $z$ , and another reason is the possible asymmetric setup of the foils.

$$[A] = \left[ \begin{array}{cccc|cccc|ccc} \cdot & \cdot & \cdot & \cdot & * & * & * & * & 0 & 0 & * & 0 \\ \cdot & \cdot & \cdot & \cdot & * & * & * & * & 0 & 0 & * & 0 \\ \cdot & \cdot & \cdot & \cdot & * & * & * & * & 0 & 0 & * & 0 \\ \cdot & \cdot & \cdot & \cdot & * & * & * & * & 0 & 0 & * & 0 \\ \hline * & * & * & * & \cdot & \cdot & \cdot & \cdot & 0 & 0 & * & 0 \\ * & * & * & * & \cdot & \cdot & \cdot & \cdot & 0 & 0 & * & 0 \\ * & * & * & * & \cdot & \cdot & \cdot & \cdot & 0 & 0 & * & 0 \\ * & * & * & * & \cdot & \cdot & \cdot & \cdot & 0 & 0 & * & 0 \\ \hline \cdot & 0 & 0 & 0 & 0 \\ \cdot & 0 & 0 & 0 & 0 \\ \cdot & 0 & 0 & 0 & 0 \\ \cdot & 0 & 0 & 0 & 0 \end{array} \right] \quad (4)$$

The draft  $z$  has an effect on both the longitudinal and lateral subset, whereas all the derivatives to  $z$  would be zero in the case of an aeroplane. This can easily be understood: An aeroplane could fly e.g. 10 m higher or lower, but this would not affect any force or moment. If the Viper from Fig. 1 would be lowered a certain distance, a larger part of the Z-boards would be submerged and this would consequently influence all force and moment terms.

If the boat experienced a certain heel  $\phi_0$  and sideslip  $v_0$ , the decoupling characteristic between the different subsets of the stability matrix ceases to be valid, as a perturbation of any form would simultaneously affect longitudinal and lateral motions. However, as the boat is meant to be sailed without any heel (this is the most efficient, i.e. fastest, way of sailing), the heel is assumed to be zero. In addition, the sideslip is very small compared to the forward velocity  $u_0$  and will also be neglected.

## 2.2 SIMPLIFICATIONS

It was mentioned earlier how this is an attempt to construct a straightforward and fast framework to support preliminary design. To further reduce the complexity of the problem, certain simplifications have to be made. These simplifications will be based on the numerical results of Masuyama, which give a solid foundation to certain intuitions. A two-phase simulation where the whole boat is included, would undoubtedly lead to more accurate results, but also to a larger mesh and calculation time. Therefore, it was chosen to only model the rudder, the elevator and the Z-board below the water surface and to assume that all forces and moments above the water surface are constant. In reality this would however not be true. The biggest contribution above the water originates from the sail. The sail will, for example, experience big variations in resulting force and moment when

the boat undergoes a roll motions and consequently this will lead to substantial stability derivatives of the sail forces and moments to the roll motion.

This immediately leads to another simplification: only *longitudinal* motions are considered, i.e. motions along the  $x$ - and  $z$ -axis and a rotation around the  $y$ -axis. An overview of the used axis-systems can be found in 3. Only longitudinal motions are considered due to the fact that the *lateral* motions are heavily affected by the sail which is modelled as a constant force and moment. The rotations around the  $z$ -axis are more of interest for a directional stability analysis. The assumption that all forces and moments above the water surface are constant is in the case of longitudinal motion justified. The effect on the sail of changing the draft or the trim angle will be next to none.

### 2.3 LONGITUDINAL STABILITY MODEL

As this model considers only one rotation, the use of the inertial earth-bound frame is more convenient than the usual stability frame to write the governing equations of motion. A view of the mentioned axis systems can be found in Fig. 3. The axis system in uppercase ( $X^eY^eZ^e$ ) is the earth-bound right-handed axis system. The other frame is called the stability frame ( $x^{b'}, y^{b'}, z^{b'}$ ), it is displayed in orange. Its origin is coincident with the centre of gravity and the speed in equilibrium conditions lies in the  $xy$ -plane. The  $Z$ -axis is chosen downwards. As only

Eq. 5.

$$\begin{cases} X = \dot{u} \\ Z = \dot{w} \\ M = I_{yy}\dot{q} \Leftrightarrow \\ w = \dot{z} \\ q = \dot{\theta} \end{cases} \begin{cases} \frac{du}{dt} = \frac{X(u, z, \theta)}{m} \\ \frac{dw}{dt} = \frac{Z(u, z, \theta)}{m} \\ \frac{dq}{dt} = \frac{M(u, z, \theta)}{I_{yy}} \\ \frac{dz}{dt} = w \\ \frac{d\theta}{dt} = q \end{cases} \quad (5)$$

The above equations are linearized using small-disturbance theory, and the forces and moment are substituted by their Taylor approximations as in Eq. 2. This then leads to Eq. 6 with  $A_r$  being the reduced stability matrix.

$$\frac{d}{dt} \begin{bmatrix} \Delta u \\ \Delta w \\ \Delta q \\ \Delta z \\ \Delta \theta \end{bmatrix} = [A_r] \cdot \begin{bmatrix} \Delta u \\ \Delta w \\ \Delta q \\ \Delta z \\ \Delta \theta \end{bmatrix} \quad (6)$$

$$[A_r] = \begin{bmatrix} \frac{1}{m} \frac{\partial X}{\partial u} & \frac{1}{m} \frac{\partial X}{\partial z} & \frac{1}{m} \frac{\partial X}{\partial \theta} & \frac{1}{m} \frac{\partial X}{\partial w}^* & \frac{1}{m} \frac{\partial X}{\partial q}^{**} \\ \frac{1}{m} \frac{\partial Z}{\partial u} & \frac{1}{m} \frac{\partial Z}{\partial z} & \frac{1}{m} \frac{\partial Z}{\partial \theta} & \frac{1}{m} \frac{\partial Z}{\partial w}^* & \frac{1}{m} \frac{\partial Z}{\partial q}^{**} \\ \frac{1}{m} \frac{\partial u}{\partial u} & \frac{1}{m} \frac{\partial u}{\partial z} & \frac{1}{m} \frac{\partial u}{\partial \theta} & \frac{1}{m} \frac{\partial u}{\partial w}^* & \frac{1}{m} \frac{\partial u}{\partial q}^{**} \\ \frac{1}{I_{yy}} \frac{\partial M}{\partial u} & \frac{1}{I_{yy}} \frac{\partial M}{\partial z} & \frac{1}{I_{yy}} \frac{\partial M}{\partial \theta} & \frac{1}{I_{yy}} \frac{\partial M}{\partial w}^* & \frac{1}{I_{yy}} \frac{\partial M}{\partial q}^{**} \\ 0 & 1 & 0 & 0 & 0 \\ 0 & 0 & 1 & 0 & 0 \end{bmatrix} \quad (7)$$

### 2.4 DERIVATIVES

The afore mentioned stability matrix needs to be constructed with numerical results for the different stability derivatives. The derivatives are calculated by finite differences constructed from the forces resulting from different CFD calculations.

The stability derivatives in the first three columns of Eq. 7 are very straightforward to calculate as they only require steady-state simulations. The stability derivatives to  $w$  and  $q$  however are more expensive to calculate using CFD as they require transient solutions. Including these expensive calculations in the framework would make it a rather unsuitable tool for preliminary design stages as the computation cost would soon become staggering. The contribution of these expensive stability derivatives to the eigenmodes of the stability matrix can however not be understated. This hypothesis was supported by the numerical stability derivatives as provided by Masuyama [4] and later also confirmed by

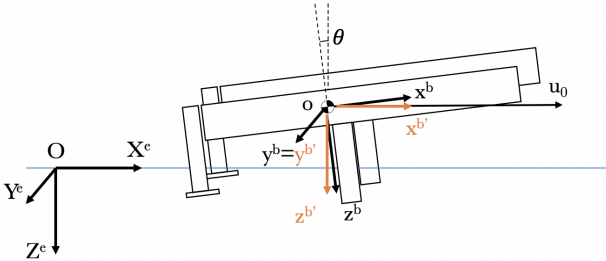


Figure 3: An overview of the used axis systems.

longitudinal motions are considered, the 6 dynamic relations of the general approach mentioned in Sec. 2.1 are reduced to only 3 relations: force balances along the  $X$  and  $Z$  direction and a moment balance around the  $y$ -axis. The moment of inertia  $I_{yy}$  and moment  $M$  are defined around the centre of gravity. These 3 dynamic relations are completed with 2 kinematic relations as shown in

the stability analysis of the Viper. That is why the terms with (\*) and (\*\*) will be approximated using the other 9 steady-state force derivatives. This will be explained in the paragraphs below. The terms denoted with (\*) in

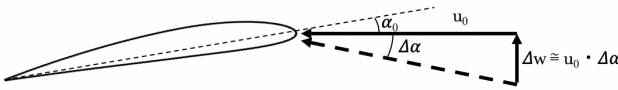


Figure 4: Effect of the vertical velocity,  $w$ .

Eq. 7 are the force and moment derivatives to the speed in the vertical direction (heave). These terms will be approximated using the derivatives to the trim angle  $\theta$ :  $\frac{\partial X}{\partial \theta}$ ,  $\frac{\partial Z}{\partial \theta}$  and  $\frac{\partial M}{\partial \theta}$ . As can be seen from Fig. 4 a perturbation  $\Delta w$  of the vertical velocity causes a change in angle of attack  $\alpha$  from the viewpoint of the foils. Since a hydrofoil boat sailing in equilibrium conditions will always have a horizontal speed, a change in trim angle  $\Delta\theta$  is seen by the foils as a change in angle of attack  $\Delta\alpha$ . The difference between changing  $\alpha$  and changing  $\theta$  lies in the fact that the submerged area differs if the trim angle is changed. However, this effect is rather small and can be neglected, i.e.  $\frac{\partial \dots}{\partial \theta} \sim \frac{\partial \dots}{\partial \alpha}$ . Assuming small disturbances around an equilibrium point,  $\frac{\partial Z}{\partial w}$  can be approximated as is shown in Eq. 8. The procedure for  $\frac{\partial X}{\partial w}$   $\frac{\partial M}{\partial w}$  is analogous.

$$\frac{\partial Z}{\partial w} = \frac{\partial Z}{\partial \theta} \frac{\partial \theta}{\partial w} \approx \frac{1}{u_0} \frac{\partial Z}{\partial \theta} \quad (8)$$

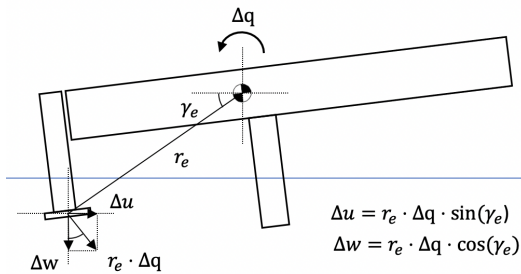


Figure 5: Effect of the pitch,  $q$ .

The terms denoted with (\*\*) in Eq. 7 are the derivatives of the forces and moment to pitch. An angular velocity  $q$  around the centre of gravity causes an additional velocity component on both foils. This velocity component can be decomposed in a horizontal and vertical part, respectively  $\Delta u$  and  $\Delta w$ , as is demonstrated in Fig. 5. This component depends on the individual positioning

of each foil. The positioning is characterised in the figure by the distance to the centre of gravity  $r_e$  and the angle in the stability frame to the horizontal plane,  $\gamma_e$ . Using the expression from Eq. 8 an approximation of  $\frac{\partial M}{\partial q}$  is developed in Eq. 9. The procedure for  $X$  and  $Z$  is analogous.

$$\begin{aligned} \frac{\partial M}{\partial q} &= \frac{\partial M}{\partial u} \frac{\partial u}{\partial q} + \frac{\partial M}{\partial w} \frac{\partial w}{\partial q} \\ &= \frac{\partial M}{\partial u} r_e \sin(\gamma_e) + \frac{\partial M}{\partial w} r_e \cos(\gamma_e) \\ &\approx \frac{\partial M}{\partial u} r_e \sin(\gamma_e) + \frac{1}{u_0} \frac{\partial M}{\partial \theta} r_e \cos(\gamma_e) \end{aligned} \quad (9)$$

Notice that this procedure has to be completed for every component separately as their individual positioning varies. Afterwards their individual derivatives are summed to obtain the total derivative necessary in the stability matrix.

These approximations for the derivatives are quite valuable as they allow to construct the stability matrix  $A$  with only a few steady-state simulations.

### 3 CFD METHODOLOGY

#### 3.1 MESH

The complete mesh will be constructed using an *overset* methodology. Oversetting allows us to create three much ‘simpler’, separate component meshes around the elevator, rudder and Z-board together with a rectangular hexahedral background mesh in which they overlap. The solver will, after initialisation, remove overlap between the different meshes by deactivating redundant cells. The background mesh can be much coarser than the component meshes as nearly no gradients will be present here. Nevertheless, special care should be taken to make sure that component meshes and background mesh have similar sizing in regions of overlap as this will give rise to better results for the overset initialisation.

Assuming a symmetric boat experiencing only *longitudinal* motions, the used geometry should only contain one half boat. This results in 1 rudder, 1 elevator and 1 Z-board as our geometry. Simulating only half of the geometry has a large beneficial influence on calculation time. The CAD-files of the Viper were provided by Goodall Design. Using these CAD-files, the three components (rudder, elevator and Z-board) are meshed sep-

arately using the *ICEM* software package from ANSYS. An example of a component mesh is shown in Fig. 6 for the elevator.

The three component meshes are all hexahedral C-grid

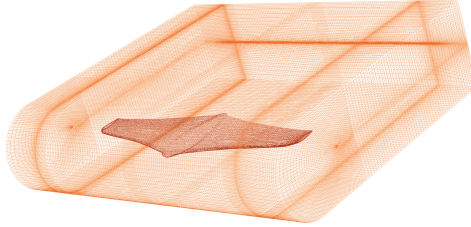


Figure 6: The elevator mesh.

meshes which are sufficiently long downstream to resolve the wake. The C-grid has a radius of only 1 chord length. The first cell of the boundary layer of all three foils is located at  $0.1 \text{ mm}$  to have a  $y^+$  value approximately between 30 and 300. An overview of the components together with the background mesh is shown in Fig. 7. It can be seen how the background mesh is refined towards the components. It was chosen to model the free surface as a *rigid lid* rather than using a multi-phase flow method as this is outside the scope of this work. The black surface in Fig. 7 represents the free surface modelled as a free-slip wall. The blue surfaces are pressure outlets which are tilted slightly at the outlet to prevent reversed flow on these surfaces. The green surface, which lies at the centre line of the boat, is modelled as a symmetry plane. This background mesh is completed with a velocity inlet and pressure outlet at the ends which are omitted in the figure. The complete mesh holds  $5.56 \cdot 10^6$  cells but which are not all *solve cells*. Due to the overset methodology locally only the smallest mesh will be solved.

### 3.2 FLOW SOLVER

As the speed range in which foiling is to be expected lies above  $5 \text{ m/s}$  and the foils have chord lengths of  $0.2 \text{ m}$ , Reynolds numbers always lie well above  $10^6$ . Turbulence is modelled using the  $k - \omega$  SST model. At the velocity inlet the turbulence intensity is set to 1% and the viscosity ratio  $\frac{\mu_t}{\mu}$  is set to 1. To include the effects of hydrostatic pressure gravity  $g$  is enabled and a hydrostatic pressure profile is imposed at the pressure outlets. The different components can be rotated and translated separately to create different setups. The reference ge-

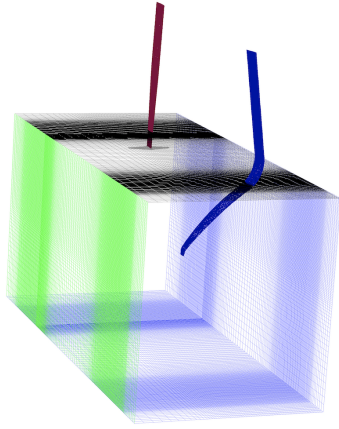


Figure 7: The components in the background mesh.

ometry<sup>1</sup> has a rudder rake of  $-1^\circ$  and a foil rake of  $4^\circ$ , with a rake defined as the relative angle of a foil to the boat.

### 3.3 Equilibrium state

As only forces and moments resulting from the foils below the water surface are calculated in CFD, other forces and moments should be estimated in order to find a realistic equilibrium state of the boat. For the force balance the weight of the boat ( $140 \text{ kg}$ ) together with the weight of the crew ( $140 \text{ kg}$ ) should be included. As only half of the boat is modelled, only half of the weight is included, resulting in a downward force of  $1.37 \cdot 10^3 \text{ N}$ . The moment generated by the sail also has to be approximated. The drag generated by the foils follows from the CFD calculations, e.g. the drag generated at forward speed of  $10 \text{ m/s}$  is equal to  $215 \text{ N}$ . The sail should deliver a force which is equal in magnitude but opposite in direction to this drag. Data provided by Goodall Design shows that the point of application of the sail lies  $3.25 \text{ m}$  above the centre of gravity. From this force and its point of application the moment can be calculated. It is worth noting that the centre of gravity is assumed to be fixed and that the boat and the crew remain non-deformable.

An algorithm to determine the equilibrium state for an arbitrary geometry and conditions was developed. A geometry can vary by changing the rudder rake, foil rake, the CoG, ... A setup can change by varying the speed of the boat. The goal of the algorithm is to find a relative trim angle  $\Delta\theta$  and relative draft  $\Delta z$  at which both the

---

<sup>1</sup>The Viper allows to change the setup of the boat by changing the rudder and board rake. This allow to setup the boat for different conditions and to alter its characteristics and behaviours.

total moment and total force on the boat are zero. This trim angle and draft are defined in reference to an arbitrary initial orientation. The algorithm is based on the *Newton-Raphson* root-finding method for 2 variables in which the new position is iteratively calculated based on the force and moment.

$$\begin{bmatrix} \Delta z_k \\ \Delta \theta_k \end{bmatrix} = J^{-1} \begin{bmatrix} -Z_k \\ -M_k \end{bmatrix}, \quad J = \begin{bmatrix} \frac{\partial Z}{\partial z} & \frac{\partial Z}{\partial \theta} \\ \frac{\partial M}{\partial z} & \frac{\partial M}{\partial \theta} \end{bmatrix} \quad (10)$$

In every step the 4 components of the Jacobian  $J$  are calculated. However if both draft and trim angle are updated simultaneously, there is no way of calculating the derivatives, as their individual contributions cannot be distinguished. That is why a segregated approach is proposed. Every iteration consists of two sub-iterations: one sub-iteration for the draft update  $\Delta z$  and one for the trim angle update  $\Delta \theta$ . Based on the Jacobian  $J_k$  an update for the draft and trim are calculated,  $\Delta z_k$ ,  $\Delta \theta_k$ . In iteration  $k + \frac{1}{2}$  the position of the boat is updated with  $\Delta z_k$ . The flow for this new orientation is solved and from the resulting new force and moment,  $Z_{k+\frac{1}{2}}$  and  $M_{k+\frac{1}{2}}$ , the derivatives to  $z$  are updated. In iteration  $k+1$  the position of the boat is updated with  $\Delta \theta_k$ . The flow for this new orientation is solved and from the resulting new force and moment,  $Z_{k+1}$  and  $M_{k+1}$ , the derivatives to  $\theta$  are updated as well. Using the Jacobian  $J_{k+1}$  new updates are calculated and the algorithm is re-iterated. This gets demonstrated in Eq. 11.

$$\begin{aligned} ① \quad & \begin{bmatrix} \Delta z_k \\ \Delta \theta_k \end{bmatrix} = J_k^{-1} \begin{bmatrix} (-Z)_k \\ (-M)_k \end{bmatrix} \\ ② \quad & \text{simulate } (z_k + \Delta z_k, \theta_k) \Rightarrow (Z_{k+\frac{1}{2}}, M_{k+\frac{1}{2}}) \\ & \rightarrow \frac{\partial Z}{\partial z} = \frac{Z_{k+\frac{1}{2}} - Z_k}{\Delta z_k}; \quad \frac{\partial M}{\partial z} = \frac{M_{k+\frac{1}{2}} - M_k}{\Delta z_k} \\ ③ \quad & \text{simulate } (z_k + \Delta z_k, \theta_k + \Delta \theta_k) \Rightarrow (Z_{k+1}, M_{k+1}) \\ & \rightarrow \frac{\partial M}{\partial \theta} = \frac{M_{k+1} - M_{k+\frac{1}{2}}}{\Delta \theta_k}; \quad \frac{\partial Z}{\partial \theta} = \frac{Z_{k+1} - Z_{k+\frac{1}{2}}}{\Delta \theta_k} \\ ④ \quad & \begin{bmatrix} \Delta z_{k+1} \\ \Delta \theta_{k+1} \end{bmatrix} = J_{k+1}^{-1} \begin{bmatrix} (-Z)_{k+1} \\ (-M)_{k+1} \end{bmatrix} \dots \end{aligned} \quad (11)$$

The algorithm was implemented in FLUENT making use of *journal files* together with *UDFs* (User-defined functions).

### 3.4 DERIVATIVES

Once the equilibrium state for a geometry and setup is found, the stability matrix needs to be constructed. The calculations for the derivatives, necessary for constructing the stability matrix, are straightforward. They are calculated with a one-sided finite difference around the equilibrium state. Together with the forces and moment from the equilibrium state (which are approximately zero), three additional sets of the forces and moment are calculated for disturbances in respectively draft, trim and surge. This is demonstrated in Eq. 12:

$$\frac{\partial A}{\partial a} = \frac{A_{\Delta a} - A_0}{\Delta a}, \quad A = X, Z, M, \quad a = \theta, z, u \quad (12)$$

with  $A_0$ , the force or moment from the equilibrium state and  $A_{\Delta a}$  the force or moment from the perturbed state.

## 4 RESULTS

The following section presents the results for the standard geometry, with an elevator rake of  $-1^\circ$  and a Z-board rake of  $4^\circ$ , at a speed of  $10 \text{ m/s}$ .

### 4.1 Equilibrium state

The equilibrium state was calculated from an arbitrary starting state. This starting state has a zero trim angle and a draft where the rudder is submerged  $100 \text{ mm}$  and the Z-board  $400 \text{ mm}$ . The position of the resulting equilibrium state relative to this starting state is defined by  $\Delta z = 159 \text{ mm}$ ,  $\Delta \theta = -2.38^\circ$ . This means that the boat moves deeper into the water and is tilted slightly *nose-down*. The rudder is now submerged  $260 \text{ mm}$  and the Z-board  $560 \text{ mm}$ .

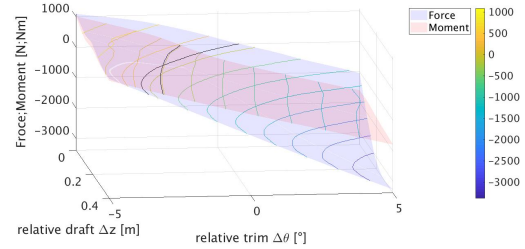


Figure 8: A surface plot of the of the force and moment of the Viper as a function of the relative draft  $z$  and the relative trim angle  $\theta$ .

In Fig. 8 a surface plot is shown of the force  $Z$  and moment  $M$  as a function of the relative draft and trim. This plot is constructed by doing a range of CFD calculations for a multitude of combinations of draft and trim. Notice that as the  $Z$ -axis is directed downwards, a *lift*-force is negative and a boat which lies deeper in the water has a more positive draft. It can be observed how the moment  $M$  depends primarily on the trim but that the force  $Z$  depends on both the trim and the draft. The two black iso-curves represent the states where the force  $Z$  or the moment  $M$  is zero. The location where the two curves intersect, is the location of the equilibrium state.

## 4.2 DYNAMIC STABILITY MATRIX

Using finite differencing, the individual derivatives of the three components (elevator, rudder and Z-board) are calculated for the draft  $z$ , trim  $\theta$  and surge  $u$ . These derivatives are then used to construct the stability matrix  $A$  for the standard geometry sailing at a speed of  $10 \text{ m/s}$ :

$$[A] = \begin{bmatrix} -0.27 & -2.21 & -4.99 & -0.50 & 0.00 \\ 0 & 0 & 0 & 1 & 0 \\ 0 & 0 & 0 & 0 & 1 \\ -2.24 & -57.20 & -156.21 & -15.62 & -6.51 \\ 0.01 & -6.42 & -78.59 & -7.86 & -14.75 \end{bmatrix}$$

Using *MATLAB*, the eigenvalues and eigenvectors of this matrix can be determined. The eigenvalues determine the general behaviour of each mode, and the eigenvectors will determine the amplitude and phase of each variable. The eigenvalues are visualised in Fig. 9 and the eigenvectors are visualised in Fig. 10, 11 and 12. From the eigenvalues and eigenvectors, the eigenmodes can be constructed:

$$\Delta x_i = v_i e^{\lambda_i t} \quad \text{with } i = 1, \dots, 5 \quad (13)$$

For a more general background on these eigenmodes on how to interpret them we refer to the work by Drela [3]. From the eigenvalues some interesting conclusions can be drawn. The first thing which can be noted is that they all have a negative real part, meaning that the boat is *dynamically stable*. Furthermore there is one real eigenvalue and two complex conjugated pairs.

By analysing the real eigenvector  $v_5$  in Fig. 10, some characteristics of the behaviour of the eigenmode  $\Delta x_5$

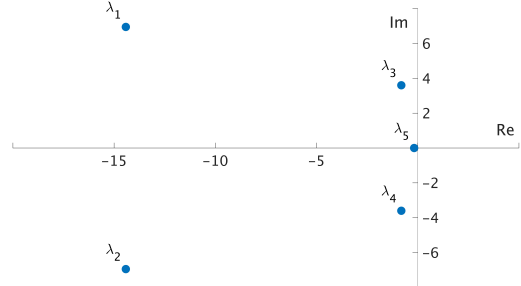


Figure 9: The root locus diagram for the standard geometry sailing at a speed of  $10 \text{ m/s}$ .

can be recognized. An increase in speed  $\Delta u$  is associated with a decrease in draft  $\Delta z$  (meaning that the boat gets lifted from the water). This corresponds to the behaviour that is expected. A draft variation  $\Delta z$  occurs naturally together with a heave variation  $\Delta w$ . As this is a real mode, this draft variation damps out without any overshoot. A half-life  $t_{\frac{1}{2}}$  is the time needed for the value to decrease by  $\frac{1}{2}$  times its original value (exponential decay). From the half-lifes it can be seen that it will take  $3.89 \text{ s}$  for this mode to lower its amplitude with  $50\%$ . This means the boat will respond quite slowly.

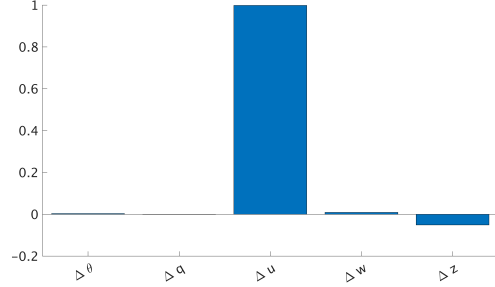


Figure 10: A visualisation of the real eigenvector  $v_5$ .

The combination of the eigenmodes  $\Delta x_1$  and  $\Delta x_2$  will be a heavily damped, sinusoidal motion dominated by a variation in heave  $\Delta w$  and pitch  $\Delta q$ . This resembles some kind of wobbling. After the boat moves downwards, it starts to tilt nose-up. This results in more lift, meaning that the boat eventually starts moving up again. Hence the oscillatory motion. The heave and pitch motion are almost in phase with each other. This mode has a half-life  $t_{\frac{1}{2};1} = t_{\frac{1}{2};2} = 4.81 \cdot 10^{-2} \text{ s}$  and a period  $T_1 = T_2 = 0.904 \text{ s}$ .

The combination of eigenmodes  $\Delta x_3$  and  $\Delta x_4$  will be

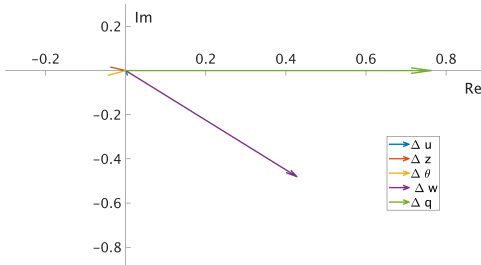


Figure 11: A visualisation of the complex eigenvector  $v_1$ .

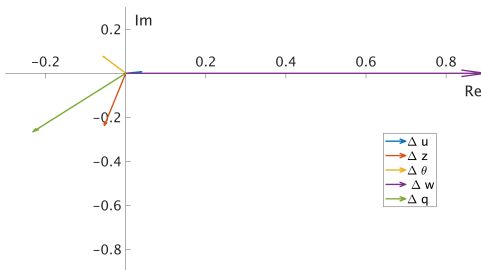


Figure 12: A visualisation of the complex eigenvector  $v_3$ .

a weakly damped, sinusoidal motion, again dominated by a variation in heave  $\Delta w$  and pitch  $\Delta q$ . The half-life is  $t_{\frac{1}{2};3} = t_{\frac{1}{2};4} = 8.54 \cdot 10^{-1}$  s and the period  $T_3 = T_4 = 1.75$  s. As the half-life and period are larger in this case, the variation in trim angle  $\Delta\theta$  and draft  $\Delta z$  resulting from the variation in heave and pitch will be more outspoken. This is demonstrated by the larger vector components for trim and draft in Fig. 12.

## 5 CONCLUSIONS

A framework for quantifying the longitudinal stability of a hydrofoil boat has been developed. This framework was applied to the Viper, from which could be concluded that this design is dynamically stable. This is also supported by sea trials.

The dynamic stability analysis definitely looks promising as a tool to be used in the design of hydrofoil crafts, just as it is a usual practice in aeroplane design. The use of CFD as the method of calculating the flow proved to be rather time consuming. As this framework is aimed to be a method to compare different designs swiftly, CFD might not be the suitable candidate to solve the forces

and moments from the flow as they prevent to make quick adjustments. Other flow calculating methods, like Prandtl's lifting-line theory or other potential flow codes might be better suited for this task. For future work it can be of interest to perform the stability analysis for more geometries to be able to compare the stability and check if the same modes reoccur. Having a more accurate model for the sail forces will allow to include lateral motions as well, to have a more complete stability analysis. Experimental data from towing tanks or full-scale tests is also key for future development of this technique.

## 6 ACKNOWLEDGEMENTS

I would like to express my gratitude to late prof. Vieren-deels who initially set everything into motion for me to propose my own thesis subject. Also I would like to thank B. Goodall and L. Verbeeck from Goodall Design for providing me with the exciting design and necessary data.

## REFERENCES

- [1] Viper classes and equipment, 2010. <https://www.sailing.org/classesandequipment/VIP.php>.
- [2] Franck cammas airlifted with serious injury, 2019. <https://www.yachtingworld.com/news/french-americas-cup-skipper-franck-cammas-badly-injured-after-being-run-over-by-foiling-catamaran-69178>.
- [3] M. Drela. *Flight Vehicle Aerodynamics*. MIT Press, 2014.
- [4] Y. Masuyama. Stability analysis and prediction of performance for a hydrofoil sailing boat. part 2: Dynamic stability analysis. *International Shipbuilding Progress*, 34:20–29, 1987.
- [5] David A. Caughey. *Introduction to aircraft stability and control*. Sibley School of Mechanical & Aerospace Engineering Cornell University, 2011.

## 7 AUTHORS BIOGRAPHY

**A. Bagué** holds the current position of PhD Student at UGent. His research is dedicated to the stability characteristics of hydrofoiling vessels. He has hands-on experience with hydrofoiling sailboats having sailed them himself. This paper was written to obtain the

degree of Master of Science in electromechanical engineering.

**E. Lataire** holds the current position of professor at Ghent University and is head of the Maritime Technology Division. He graduated in 2004 at Delft University of Technology and obtained his PhD at Ghent University in 2014. His research focuses mainly on the manoeuvring behaviour of ships in shallow and confined water and is often based upon model tests carried out in the confined water towing tank of Flanders Hydraulics Research (Antwerp, Belgium).

**T. Demeester** holds the current position of PhD student at UGent. He is working on numerical methods for fast calculation of steady state free surface flows around ships and hydrofoils. He has past experience with dynamic stability calculations for aeroplanes.

**J. Degroote** holds the current position of associate professor at the department of Electromechanical, Systems and Metal Engineering. He focuses on computational fluid dynamics and fluid-structure interaction.